ELSEVIER

International Journal of Mass Spectrometry 220 (2002) 183–192

International Journal of Mass Spectrometry

www.elsevier.com/locate/ijms

Strong fragmentation of large rare gas clusters by high energy electron impact

Stefan Schütte[1], Udo Buck*

Max-Planck-Institut für Strömungsforschung, Bunsenstraße 10, D-37073 Göttingen, Germany

Received 10 October 2001; accepted 21 January 2002

Abstract

The interaction of large argon, krypton, and xenon clusters in the size range from $\langle n \rangle = 170$ to 10,280 with electrons is investigated in a reflectron time-of-flight mass spectrometer. The clusters are generated in adiabatic expansions through conical nozzles and are nearly fragmentation-free detected by single photon ionization after they have been doped by one sodium atom. In contrast, using electron impact ionization, the clusters are nearly completely fragmented when varying the electron energy between 50 and 1500 eV. The operating mechanism is that which is also responsible for the electronic sputtering of solid matter. The yields, however, are orders of magnitude larger for clusters than for the solid. This result is a consequence of the finite dimensions of the clusters which cannot accommodate the energy. (Int J Mass Spectrom 220 (2002) 183–192)

Keywords: Rare gas cluster; Fragmentation; Electron impact; Sputtering

1. Introduction

The fragmentation of clusters after the interaction with electrons or high power photons is a well-studied subject [1,2]. Specifically, the ionization process of weakly bound systems has been investigated in great detail. For electrons with energies much above the threshold (70 eV), a small part of the excess energy is distributed over the cluster and leads to the evaporation of mainly monomers. But even close to the threshold appreciable fragmentation occurs, since the ions formed by charge localization have a much larger bonding energy of about 1 eV and are shifted to smaller equilibrium values compared to their neutral precursors so that this vibrational energy is available [3]. For small Ar_n clusters [4] and a series of molecules [5], the amount of fragmentation has been measured using size selected neutral clusters by atomic beam deflection. For argon trimers and tetramers, the experimental results are in nice agreement with recent semi-quantal dynamical calculation where all nine potential surfaces involved were coupled [6]. For clusters $n \geq 20$ we used statistical models to predict the fragmentation. They proved to be valid in the interpretation of the decay of prepared ionic clusters [7] and when combined with a realistic determination of the amount of energy left in the cluster [8] should give reasonable results. These simulations predict that the effect of fragmentation is largest for small clusters and becomes less and less important for larger clusters [8,9].

Recently, we have carried out measurements, however, in which even large clusters up to $\langle n \rangle = 10{,}000$

* Corresponding author. E-mail: ubuck@gwdg.de
[1] Present address: Agilent Technologies, 76337 Waldbronn, Germany.

1387-3806/02/$ – see front matter
PII S1387-3806(02)00670-X

were nearly completely destroyed by the interaction with electrons of energies up to 1.5 keV. We will report in this contribution the results for the rare gas clusters Ar_n, Kr_n, and Xe_n. Similar results have been obtained for $(H_2O)_n$ and $(NH_3)_n$ clusters [10] and also in the interaction with photons [11]. We note that we are not in a regime in which Coulomb explosion of the clusters occurs [12,13]. We also do not measure the fragment size distribution on an event to event basis using multi-coincidence techniques [14,15]. We are more interested in the gross features of the fragmentation process in a special collision energy regime. As we will demonstrate the conditions of our experiments resemble much more those of another well established field, the electronic sputtering of solid material [16,17]. Here, the photon, electron or fast ion impinging on the solid deposits its energy in electronic excitations of the atoms or molecules of the solid material. When this energy is rapidly dispersed in these insulators, it may be coupled to the atomic motions and then transported to the surface. Finally, the atoms or molecules escape depending on the binding energy. The measured and calculated yields per incident particle are in the range of 2–20 [18,19]. The values which have been obtained in the present experiments for clusters are orders of magnitude larger, although the mechanism of the excitation is apparently very similar. We note that we only consider here the interaction of one electron with the cluster.

The paper is organized as follows. First, we will describe the experimental apparatus, the reflectron time-of-flight mass spectrometer with the pulsed cluster source and the pulsed electron beam for ionization. For measuring the nearly fragmentation-free reference size distribution of the clusters, they are doped with one sodium atom and then photoionized. Then the results are presented in the next section and interpreted in the discussion section which follows.

2. Experimental

2.1. Vacuum system

The experiments were carried out in a multi purpose molecular beam apparatus which consists of a source chamber, a buffer chamber, and a detector unit. In the present experiment, the cluster beam is generated by adiabatic expansion and detected in a reflectron (RE) time-of-flight (TOF)-mass spectrometer. A vertical cross section of the machine is shown in Fig. 1. The source chamber (1) has a diameter of 500 mm which allows us to install various cluster beam sources. In order to have better access to the sources the front part was kept at a diameter of 200 mm. This chamber is pumped by a diffusion pump (6000 L/s) and a combination of a rootblower (500 m^3/h) and a mechanical pump (65 m^3/h). The purpose of the buffer chamber,

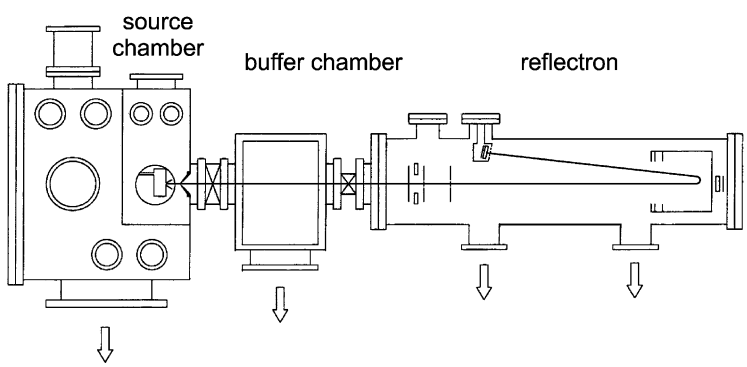

Fig. 1. Side view of the molecular beam apparatus.

that is pumped by a turbo-molecular pump (500 L/s) and a forepump, is to reduce the background pressure in the ion source of the RETOF mass spectrometer. We have chosen the linear arrangement of cluster source and reflectron in order to increase the sensitivity at the expense of mass resolution and pressure problems. The reflectron is pumped by two turbo-molecular pumps (500 and 60 L/s) and a forepump. The pressures obtained in the three chambers under operating conditions are 5×10^{-3}, 5×10^{-5}, and 5×10^{-6} mbar, respectively.

2.2. Cluster sources

The machine is equipped with a piezo-driven pulsed molecular beam source which follows a design proposed in the literature [20]. With short rise times (50 μs) and opening times between 100 and 400 μs this source provides a stable performance with constant intensity. For details we refer to [21].

In order to produce large clusters a nozzle of conical shape is used with a diameter of 350 or 600 μm, an opening angle of $2\alpha = 36^\circ$, and a length of 7.0 mm. The pressure varied between 0.3 and 10 bar at temperatures of 285–310 K.

For a reliable and simple detection, the clusters are doped by one sodium atom. The experimental arrangement is shown in Fig. 2. The temperature of the heated sodium beam source is set in such a way that, according to the vapor pressure, mainly one atom is captured by the cluster. Since this process follows a Poisson distribution, the required conditions can easily be met. Under our experimental conditions the amount of dimers never exceeded 5%.

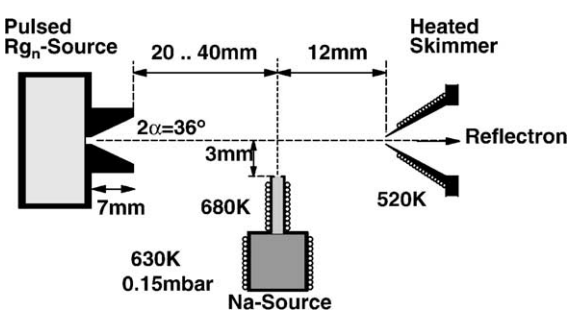

Fig. 2. Schematic view of the pick-up arrangement.

2.3. Reflectron

The heart of the machine is the reflectron. It follows the standard design criteria of modern instruments for normal applications [22,23]: a pulsed laser for ionization, a reflector without grids [24] and a long retarding field [25], and a long drift space [26]. The reflector avoids transmission losses at the meshes and introduces some geometrical focusing.

The design of the ion source allows us to simultaneously use laser photons and electrons for ionization. For the generation of the electrons a pair of copper electrodes is placed perpendicular to the cluster beam. The electron pulses are produced by the impact of the laser photon pulse on the lower copper electrode and the electrons are accelerated towards the upper electrode. This is an improved version of a previously published arrangement [27] where a Ta wire is hold in place directly in the beam. By applying suitable pulsed voltages at the two copper electrodes, based on simulations with the SIMION program, we obtain a reliable electron source with variable energy in the range from 50 to 1500 eV, a pulse width of 12 ns and currents between 10 and 300 mA. Further details of this design can be obtained from [21]. The mass resolution of the reflectron TOF was at best $m/\Delta m = 1600$ at a mass of 200 U based on the drift length of 1820 mm. This result was obtained under optimal conditions which were not always reached in the experimental results that will follow in this contribution.

The ions are extracted in the direction of the beam and detected by a microsphere plate. The photon pulses are generated by an ArF-excimer laser (Lambda Physik LPX100) at 193 nm (6.42 eV) with a pulse width of 20 ns and a pulse energy reduced to 15 mJ. We note that the same laser is used for the photoionization of the cluster and the generation of the electrons.

The mass spectra are detected using a digital storage oscilloscope in a special particle counting mode. The spectra were corrected for the size dependence of the

detection probability and the transformation from time to mass coordinates.

3. Results

A typical mass spectrum that is obtained when Xe_n clusters doped with Na atoms are photoionized is presented in Fig. 3. Here, a conical nozzle with a diameter of 350 μm, an opening angle of $2\alpha = 36^\circ$, and a length of 7.0 mm is used at a temperature of $T = 308$ K. Depending on the pressure, the size distributions exhibit a well developed maximum which is shifted to larger values with increasing source pressure. It is very well represented by a log-normal distribution

$$f(n) = \frac{1}{\sqrt{2\pi}\sigma n}\exp\left[-\frac{(\ln n - \mu)^2}{2\sigma^2}\right] \quad (1)$$

with the two parameters μ, the logarithm of the geometric mean, and σ, the logarithm of the geometric standard deviation. It is well known that large clusters follow such a log-normal distribution, if their production is caused by coagulation of larger entities and not by monomer addition. The solid lines are fits of Eq. (1) to the experimental data and the resulting average cluster sizes $\langle n \rangle$ are also indicated in Fig. 3. This method provides a simple and reliable means to ionize rare gas clusters with an as small as possible amount of fragmentation. Xenon does not absorb at all in this energy range and the power of the laser was varied in order to exclude multiphoton absorptions. There is still the possibility that a few atoms evaporate during the ionization process. A rough estimate of this number that does not take into account any change of the potential energy surfaces gives the result as follows. With a photon energy of 6.14 eV and an ionization potential of Na of 5.13 1.29 eV are left to be distributed in the cluster. With a bonding energy of 143 meV of a xenon atom the maximal number of evaporating Xe atoms is 9. A similar value for Ar would be 16. These values do not really influence the interpretation of the results in the size range studied here.

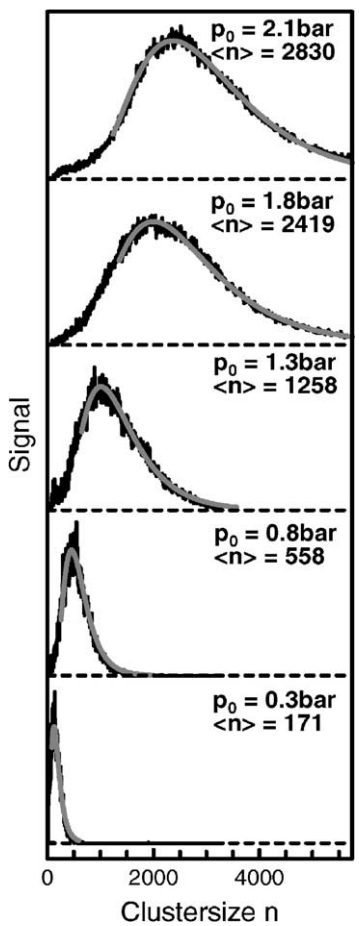

Fig. 3. Measured mass spectra of Na doped Xe_n clusters at the source pressures indicated detected by photoionization. The sizes are determined from the fitted log-normal distributions specified by the solid lines.

Similar results as those obtained for Xe_n clusters have been observed for Kr_n and Ar_n clusters. An example for Kr_n is shown in Fig. 4. Again we find a large variation of the sizes as function of the source pressure. As expected from the smaller binding energy, the average cluster size decreases in comparison with Xe_n using the same source conditions.

Now we have repeated the experiments for Kr_n clusters replacing the photons by 750 eV electrons. The results are shown in Fig. 5. The shape of the curves looks very similar and can also be fitted by log-normal distribution. The average cluster sizes, however, are very much smaller. In the case of the source pressure $p = 10$ bar it drops from $\langle n \rangle = 7027$ to $\langle n \rangle = 1269$. Obviously, there is an appreciable

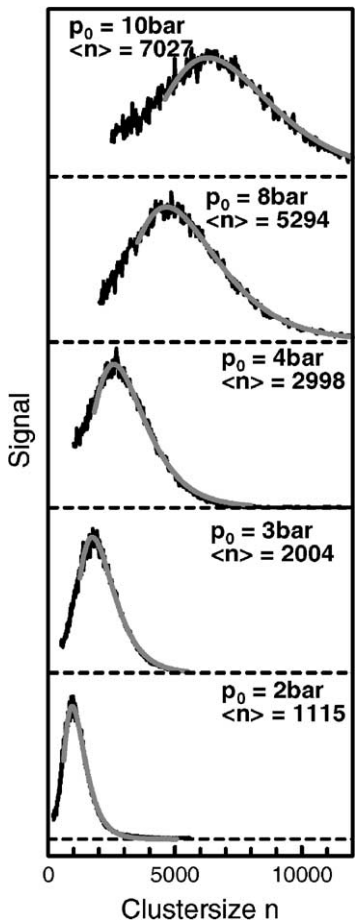

Fig. 4. Measured mass spectra of Na doped Kr_n clusters at the source pressures indicated and detected by photoionization. The sizes are determined from the fitted log-normal distributions specified by the solid lines.

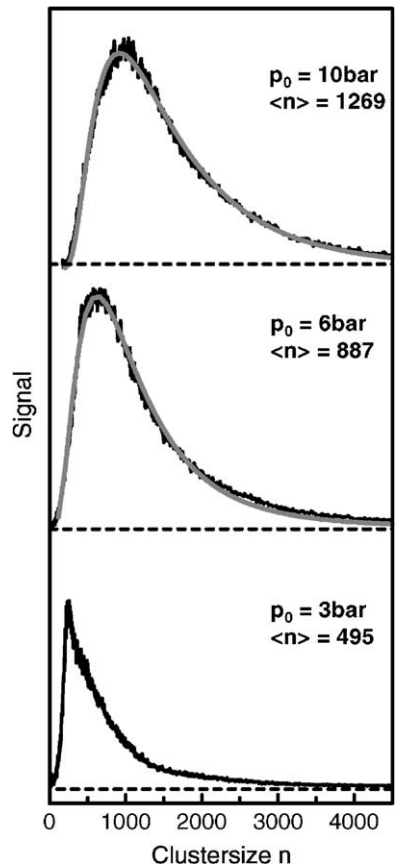

Fig. 5. Measured mass spectra of Kr_n clusters at the source pressures indicated and detected by electron impact at 750 eV. The sizes are determined from the fitted log-normal distributions specified by the solid lines.

amount of fragmentation that occurs in the interaction with electrons. We also note that the statement that the existence of a log-normal distribution is an indication of a fragmentationless behavior, is definitely wrong, since both distributions, with and without fragmentation obey the same distribution function.

In the case of electron impact ionization, we have to account for another effect that influences the measured size distributions, the appearance of multiply charged products. These were observed in many experiments [28–30] and the critical appearance sizes for the doubly charged rare gas clusters are 91 for Ar_n, 69 for Kr_n, and 49 for Xe_n clusters [31,32]. Thus, mainly the doubly charged products might be able to influence the size distributions, since the amount of the higher charged fragments is usually too small [29]. In fact, we observed explicitly the appearance of doubly charged ions in another experiment for water clusters [10] with a threshold value of 37, in close agreement with earlier experiments [30]. Because of the lower mass to charge ratio of the doubly charged products, the size distribution is shifted to smaller values. To correct for this effect, we applied the following procedure. We assume that also the doubly charged clusters follow a log-normal distribution and, instead of fitting one we fitted two log-normal distributions to the

experimental data, one of which has the half average value of the other. If we applied this procedure to the rare gas clusters, we found an amount of at most 5% doubly charged clusters. The average values of singly ionized sizes were determined to be at most 2% larger than those that were fitted by one distribution only. In the case of Kr_n in the upper part of Fig. 5 the average size changed from $\langle n \rangle = 1269$ to $\langle n \rangle = 1278$. Thus, we neglected this correction, but we have to keep in mind this result in the following discussion.

In order to quantify this strong fragmentation, we have measured mass spectra for Ar_n, Kr_n, and Xe_n clusters under exactly the same source conditions both for 6.42 eV photons and electrons with the energies

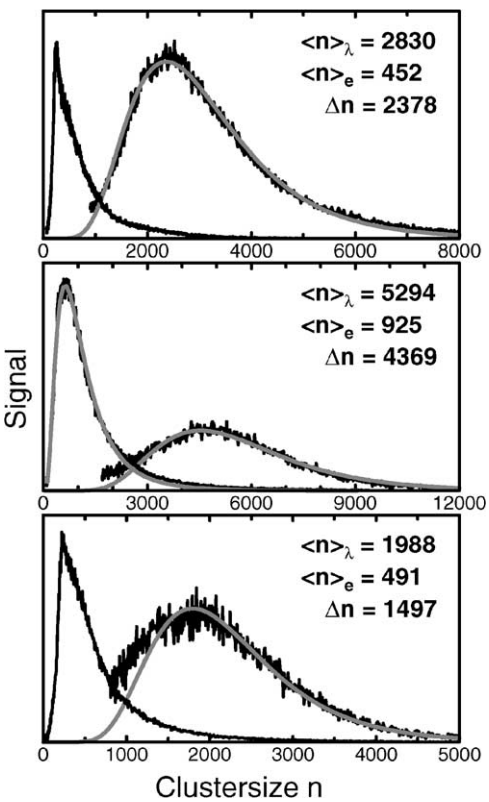

Fig. 6. Measured mass spectra of the rare gas clusters Xe_n (top), Kr_n (middle), and Ar_n (bottom), obtained under the same source conditions, but detected by photoionization and by electron impact at the energies 800, 750, and 400 eV, respectively. The sizes are determined from the fitted log-normal distributions specified by the solid lines.

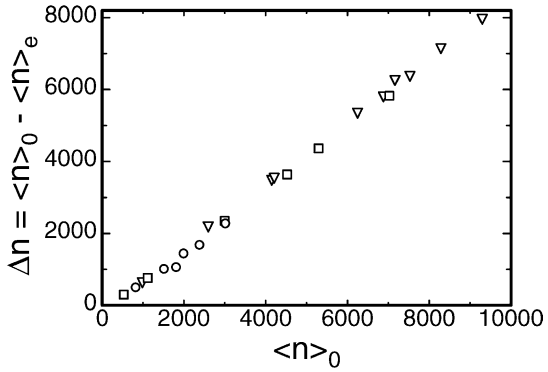

Fig. 7. Number of evaporated atoms as function of the initial cluster size for Ar (○), Kr (□), and Xe (▽).

400, 750, and 800 eV, respectively. For these energies the amount of fragmentation is largest. The result is shown in Fig. 6. We define the number of evaporated atoms by

$$\Delta n = \langle n \rangle_0 - \langle n \rangle_e \quad (2)$$

where $\langle n \rangle_0 = \langle n \rangle_\lambda$ is the average cluster size measured for photons and $\langle n \rangle_e$ that measured for electrons. The numbers Δn vary from 1497 to 4369 and indicate a massive loss of particles. The dependence of the number of evaporated atoms Δn from the original size $\langle n \rangle_0$ is plotted in Fig. 7. Surprisingly, a linear behavior results, that is the fragmentation increases with increasing cluster size. We note that the slope is the same for the three rare gases.

This behavior is in complete contrast of what has been discussed in the introduction about the interaction of a low energy electron with small clusters. By this mechanism the fragmentation should decrease with increasing cluster size, since the increasing amount of available degrees of freedom can easier accommodate the energy deposited in the cluster caused by the molecular rearrangement upon ionization.

4. Discussion

Apparently, the linear dependence of the number of evaporated atoms from the cluster size suggests that the electron interacts in a multiple way with the

cluster. The energy release per each event might be constant and independent from the size so that the increase simply results from the increase of events. In order to get more insight into this hypothesis, the energy dependence of the fragmentation was measured. The result is shown in Fig. 8 for three characteristic sizes of Ar_n, Kr_n, and Xe_n. The curves exhibit the same characteristic behavior. They sharply rise to a maximum and then level off with increasing electron energy. The maximum occurs at 400 eV for argon, at 750 eV for krypton, and 710 eV for xenon. This behavior is very well known to occur for the stopping power that charged particles experience when they penetrate into a solid. We have calculated the stopping cross section $S = (dE/ds)/\rho$, the energy loss per unit path length and density (atoms per volume), for electrons interacting with the three rare gases.

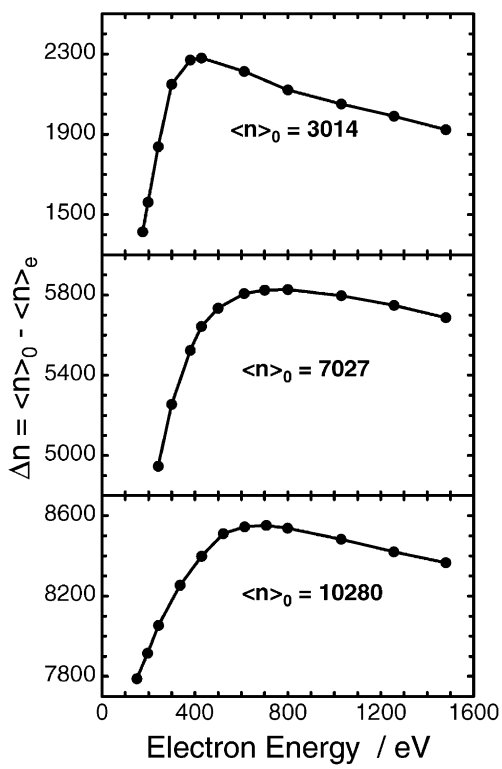

Fig. 8. Measured energy dependence of the number of evaporated atoms after electron impact of Ar_n (top), Kr_n (middle), and Xe_n (bottom) clusters. The maxima occur at 400, 750, and 710 eV, respectively.

Table 1
Sputtering yields (Y) for rare gas clusters after electron impact

Rare gas	$\langle n \rangle$	Energy (eV)	Y
Ar	3014	400	2280
Kr	4525	700	3638
Kr	7027	700	5827
Xe	7163	700	6251
Xe	10280	700	8560

This is not a standard procedure, since the Bethe formula of the text books is only valid in the large energy regime. On the other hand, direct data in the low energy regime for electrons impinging on the heavy rare gases are quite rare [33]. Thus, we follow the procedure to convert the well measured data for the proton stopping power [34] to the electron stopping power by looking for data taken at the same velocity [35]. In the article of Greene and Peterson [35] this procedures has been carried out for a series of datasets and we use in what follows their explicit parametrization for the rare gases given in Table 1 and Fig. 6 of [35].

The result for the three rare gases is shown in Fig. 9. The agreement with the measured energy dependence is amazing. The positions of the maxima are a little bit shifted to smaller values but the general shape is quite well reproduced. This agreement suggests that probably the same mechanisms operate in clusters in the studied energy regime as are observed

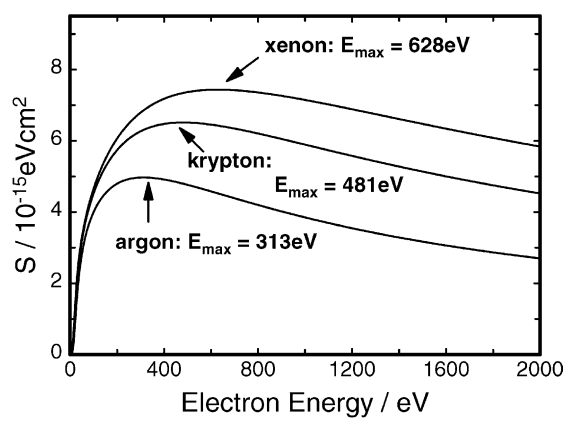

Fig. 9. Calculated stopping cross sections for the solid rare gases Ar, Kr, Xe using [34].

in the sputtering of solids under the attack of charged particles.

Sputtering of solids is a very well studied and mature field and we will briefly review here some of the main results [16,17]. The sputtering of these weakly bound insulator material is dominated by electronic interactions and consists of three separate processes. First, the incoming particle interacts with the target and produces electronic excitations and ionizations along the track. Second, these excitations or electron-hole pairs deposit energy into the solid as a result of non-radiative relaxations or repulsive decays which appear as kinetic energy of the atoms. This energy has to be transported back by collisions to the surface where, finally, the particles evaporate. In the regime of low excitation density, the yield, the number of ejected particles per incoming electron or charged particle, is written as $Y = \Delta z/\lambda_e$ in which λ_e is the mean spacing between excitations and Δz is the mean depth from which an excitation can lead to ejection weighted over possible ejection processes. The single charged particle produces a track of excitations and ionizations along its path through the solid. Here, we have $\lambda_e^{-1} = (dE/ds)/W$, where (dE/ds) is the electronic stopping power and W the averaged energy deposited in the solid which is effective for the sputtering. The Δz is determined by the kinetic energy release to the target ΔE, the cohesive energy of the solid U and a characteristic distance l between the atoms giving $\Delta z = cl\,\Delta E/U$. The constant c is 0.1–0.2 as shown in molecular dynamics simulations [36]. The distance l is either the spacing between two atomic layers or is obtained from the reciprocal of the density and the collision cross section. Thus, the yield is given by

$$Y = c\frac{l}{U}\Delta E\left(\frac{dE}{ds}\right)\frac{1}{W}. \tag{3}$$

In many cases the yield for the solid material is indeed found to be proportional to the stopping power. In some cases which are dominated by diffusion processes the maximum in the yield is at energies for which the primary electrons have a range comparable to the diffusion length which is in the order of 20–30 nm [19]. In all cases the measured and calculated yields are in agreement and are found in the order of 2–4 for the solid rare gases.

The results for the clusters clearly demonstrate that in case of electron bombardment the yield is always directly correlated with the stopping power (dE/ds). Figs. 8 and 9 demonstrate convincingly the similarity of the results. Here, the calculated stopping cross sections $S = (dE/ds)/\rho$ with the density ρ are plotted and compared with the measurement of the number of evaporated atoms Δn that is in the language of the sputtering community equal to the yield Y, the number of ejected particles per incoming projectile. Thus, we conclude that the mechanisms which lead to the fragmentation of the clusters are very similar as in electronic sputtering of the corresponding solids.

It comes as a surprise when one considers the yield. In case of the solids, the yield in the linear regime is always, calculated and measured, between 1 and 5 whatever conditions are chosen. Here, we find for the clusters at least two orders of magnitude larger values. Characteristic results for the yield are given in Table 1 together with the relevant data of the cluster and the electron beam. Simple geometric considerations of the larger surface area of clusters cannot explain these large differences. We think that the reason for this discrepancies is the finite dimension of the latter ones. The diameter of the clusters listed in Table 1 reaches from 3.0 to 5.2 nm. That means that the second part of the sputtering model in solids, the transport of the energy to the surface, does not play any role in clusters. This is nicely demonstrated if we calculate the distribution of heat in such a material. During the penetration of the electrons through the matter the primary electronic excitation and ionization processes lead by electron–phonon interaction to the vibrational excitations of the target atoms. The spread of the energy can be described by the heat equation of a temperature field $T(t, r)$ which is a function of the time t and the spatial coordinate r. The solution of the linear heat equation for a point source with the released energy H is [37]

$$T(r, t) = \frac{H}{\rho c_p (4\pi Dt)^{3/2}}\exp\left(-\frac{r^2}{4Dt}\right) \tag{4}$$

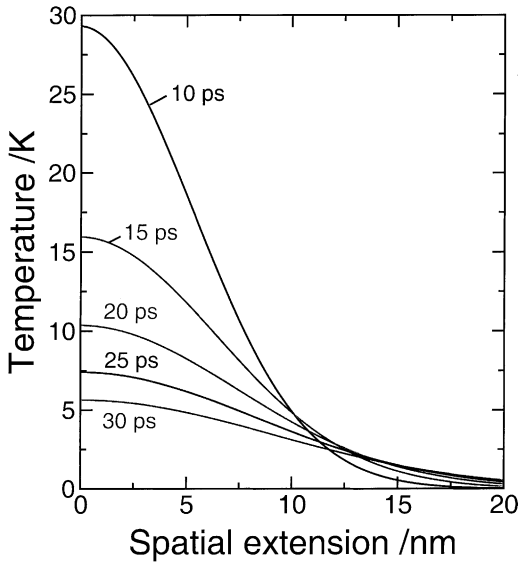

Fig. 10. Calculated temperature spatial distribution for the indicated times after the excitation of solid Ar with 400 eV.

with the density ρ, the specific heat at constant pressure c_p, and the heat diffusivity D which is related to the thermal conductivity λ by $D = \lambda/\rho c_p$. It is interesting to note that the same equation is also used for describing the heat distribution in laser ablation [38]. We calculated the spread of the energy distribution for different times according to Eq. (4) for solid argon using the published material parameters [39]. The result is presented in Fig. 10. Already after 10 ps the energy spreads over about 15 nm and the heat disappears. This is, of course, completely irrelevant for a solid of normal dimensions. Our investigated clusters, however, are still smaller. Obviously the cluster cannot accommodate the excitation energy and nearly evaporates completely. That is exactly what we observe. Here the cluster behaves differently in a size range in which other physical and chemical properties adopt already the behavior of the solid.

We conclude that the interaction of large rare gas clusters with electrons in the energy range between 100 and 1500 eV is dominated by processes which are well known from the sputtering of the corresponding solids. The charged particle produces electronic excitations and electron-hole pairs along the track which deposit energy into the vibrational motion of the cluster atoms. Therefore the energy dependence follows the stopping cross section and the yield of evaporated atoms increases with increasing cluster size. In contrast to the behavior of the solids, the heat spreads fast over the complete cluster which cannot anymore accommodate the energy and nearly completely evaporates.

Acknowledgements

The work was supported by the Deutsche Forschungsgemeinschaft in SFB 357. We acknowledge the useful discussions with T.D. Märk, J. Schou, and M. Faubel on the sputtering problem and thank M. Hobein for building the first version of the reflectron. We are grateful to C. Steinbach for helpful discussions and the preparation of the figures. Last we thank the two referees for their illuminating comments, in particular that one who helped us to understand the intricate problems that arise in the correct reproduction of the stopping power.

References

[1] H. Haberland (Ed.), Clusters of Atoms and Molecules, Springer, Berlin, 1994.
[2] T.D. Märk, in: L.G. Christopherou et al. (Eds.), Linking the Gaseous and Condensed Phases of Matter, Plenum Press, New York, 1994, p. 155 and references cited therein.
[3] H. Haberland, Surf. Sci. 156 (1985) 305.
[4] U. Buck, H. Meyer, J. Chem. Phys. 84 (1986) 4854.
[5] U. Buck, J. Phys. Chem. 92 (1988) 1023.
[6] A. Bastida, N. Halberstadt, J.A. Beswick, F.X. Gadéa, U. Buck, R. Galonska, C. Lauenstein, Chem. Phys. Lett. 249 (1996) 1.
[7] Y. Ji, M. Foltin, C.H. Liao, T.D. Märk, J. Chem. Phys. 96 (1992) 3624.
[8] P. Lohbrandt, R. Galonska, H.J. Kim, M. Schmidt, U. Buck, in: R. Campargue (Ed.), Advances in Molecular Beams, Springer, Berlin, 2000, p. 623.
[9] R. Karnbach, M. Joppien, J. Stapelfeld, J. Wörmer, T. Möller, Rev. Sci. Instrum. 64 (1993) 2838.
[10] C. Bobbert, S. Schütte, C. Steinbach, U. Buck, Eur. Phys. J. D 19 (2002) 183.
[11] S. Schütte, U. Buck, Appl. Phys. A 69 (1999) S209.

[12] T. Ditmire, J.W.G. Tisch, E. Springate, M.B. Mason, N. Hay, R.A. Smith, J. Marangos, H.R. Hutchison, Nature 386 (1997) 54.
[13] M. Lezius, S. Dobosz, D. Normand, M. Schmidt, Phys. Rev. Lett. 80 (1998) 261.
[14] B. Farizon, M. Farizon, M.J. Gaillard, F. Gobet, G. Guillermier, M. Carré, J.P. Buchet, P. Scheier, T.D. Märk, Phys. Rev. Lett. 81 (1998) 4108.
[15] B. Farizon, M. Farizon, M.J. Gaillard, F. Gobet, M. Carré, J.P. Buchet, P. Scheier, T.D. Märk, Eur. Phys. Lett. 5 (1999) 5.
[16] R.E. Johnson, B.U.R. Sundquist, Physics Today, March (1992) 28.
[17] R.E. Johnson, J. Schou, Mat. Fys. Medd. Dan. Vid. Selsk. 43 (1993) 403.
[18] R.E. Johnson, M. Pospieszalka, W.L. Brown, Phys. Rev. B 44 (1991) 7263.
[19] O. Ellegaard, R. Pedrys, J. Schou, H. Sørensen, P. Børgesen, Appl. Phys. A 46 (1988) 305.
[20] D. Proch, T. Trickl, Rev. Sci. Instrum. 60 (1989) 4.
[21] S. Schütte, Max-Planck-Institut für Strömungsforschung, Report 7 (1997), Ph.D. Thesis, University of Göttingen, 1996.
[22] H. Haberland, in: H. Haberland (Ed.), Clusters of Atoms and Molecules, Vol. 1, Springer, Berlin, 1994, p. 241.
[23] U. Boesl, R. Weinkauf, C. Weickhardt, E.W. Schlag, Int. J. Mass. Spectrom. Ion. Proc. 131 (1994) 87.
[24] R. Frey, G. Weiss, H. Kaminski, E.W. Schlag, Z. Naturforsch 40 (1985) 1349.
[25] T. Bergmann, T.P. Martin, H. Schaber, Rev. Sci. Instrum. 61 (1990) 2592.
[26] B.A. Mamyrin, V.I. Karataev, D.V. Shmikk, V.A. Zagulin, Sov. Phys. JETP 37 (1973) 45.
[27] E.R. Rohwer, R.C. Beavis, C. Köster, J. Lindner, J. Grotemeyer, E.W. Schlag, Z. Naturforsch 43 (1988) 1151.
[28] K. Sattler, J. Mühlbach, O. Echt, P. Pfau, E. Rechnagel, Phys. Rev. Lett. 47 (1981) 160.
[29] P. Scheier, T.D. Märk, , Intern. J. Mass Spectrom. Ion Proc. 76 (1987) R11.
[30] O. Echt, T.D. Märk, in: H. Haberlanr (Ed.), Clusters of Atoms and Molecules, Vol. 2, Springer, Berlin, 1994, p. 183.
[31] P. Scheier, G. Walder, A. Stamatovic, T.D. Märk, J. Chem. Phys. 90 (1989) 4091.
[32] M. Lezius, P. Scheier, A. Stamatovic, T.D. Märk, J. Chem. Phys. 91 (1989) 3240.
[33] S. Valkealahti, J. Schou, R.M. Nieminen, J. Appl. Phys. 65 (1989) 2258.
[34] W. Whaling, Encyclopedia of Physics, Vol. 34, Springer, Berlin, 1958, p. 193.
[35] A.E.S. Green, L.R. Peterson, J. Geophys. Res., Space Phys. 73 (1968) 233.
[36] S. Cui, R.E. Johnson, P. Cummings, Surf. Sci. 207 (1988) 186.
[37] U. Grigull, H. Sandner, Wärmeleitung, Springer, Berlin, 1979, p. 105.
[38] W. Bräuchle, Thermal, Photophysical, and Photochemical Processes, Springer, Berlin, 1993, p. 19.
[39] M.L. Klein, J.A. Venables (Eds.), Rare Gas Solids, Academic Press, London, 1976.